Available online at www.sciencedirect.com
SCIENCE DIRECT®
ELSEVIER
Deep-Sea Research I 52 (2005) 861–880
DEEP-SEA RESEARCH PART I
www.elsevier.com/locate/dsr

# Latitudinal distribution of microbial plankton abundance, production, and respiration in the Equatorial Atlantic in autumn 2000

Valesca Pérez[a,*], Emilio Fernández[a], Emilio Marañón[a], Pablo Serret[a], Ramiro Varela[a], Antonio Bode[b], Manuel Varela[b], Marta M. Varela[b], Xosé Anxelu G. Morán[c], E. Malcolm S. Woodward[d], Vassilis Kitidis[e], Carlos García-Soto[f]

[a]*Departamento de Ecoloxía e Bioloxía Animal, Facultade de Ciencias do Mar, Universidade de Vigo, Ctra. Colexio Universitario s/n, E-36310 Vigo, Spain*
[b]*Centro Oceanográfico de A Coruña, Instituto Español de Oceanografia, Muelle de Ánimas, Apdo. 130, E-15080A Coruña, Spain*
[c]*Centro Oceanográfico de Xixón, Instituto Español de Oceanografia, Camín de L'Arbeyal s/n, E-33212 Xixón, Asturies, Spain*
[d]*Plymouth Marine Laboratory, Prospect Place, West Hoe, Plymouth PL1 3DH, UK*
[e]*University of Newcastle, Depart. of Marine Sciences and Coastal Management, Newcastle upon Tyne NE1 7 RU, UK*
[f]*Instituto Español de Oceanografía, Centro Oceanográfico de Santander, Apdo. 240, E-39080 Santander, Spain*

Received 15 April 2004; received in revised form 16 November 2004; accepted 3 January 2005

**Abstract**

Phytoplankton and bacterial abundance, size-fractionated phytoplankton chlorophyll-*a* (Chl-*a*) and production together with bacterial production, microbial oxygen production and respiration rates were measured along a transect that crossed the Equatorial Atlantic Ocean (10°N–10°S) in September 2000, as part of the Atlantic Meridional Transect 11 (AMT 11) cruise. From 2°N to 5°S, the equatorial divergence resulted in a shallowing of the pycnocline and the presence of relatively high nitrate ($>1\,\mu M$) concentrations in surface waters. In contrast, a typical tropical structure (TTS) was found near the ends of the transect. Photic zone integrated $^{14}C$ primary production ranged from ~200 mg $C\,m^{-2}\,d^{-1}$ in the TTS region to ~1300 mg $C\,m^{-2}\,d^{-1}$ in the equatorial divergence area. In spite of the relatively high primary production rates measured in the equatorial upwelling region, only a moderate rise in phytoplankton biomass was observed as compared to nearby nutrient-depleted areas (22 vs. 18 mg Chl-*a* $m^{-2}$, respectively). Picophytoplankton were the main contributors (>60%) to both Chl-*a* biomass and primary production throughout the region. The equatorial upwelling did not alter the phytoplankton size structure typically found in the tropical open ocean, which suggests a strong top-down control of primary producers by zooplankton. However, the impact of nutrient supply on net microbial community metabolism, integrated over the euphotic layer, was evidenced by an average net microbial community production within the equatorial divergence (1130 mg $C\,m^{-2}\,d^{-1}$) three-fold larger than net production measured in the TTS region (370 mg $C\,m^{-2}\,d^{-1}$). The entire region under study showed net autotrophic community

*Corresponding author. Tel.: +34 986 814087; fax: +34 986 812556.
*E-mail address:* vperez@uvigo.es (V. Pérez).

0967-0637/$ - see front matter 
doi:10.1016/j.dsr.2005.01.002

metabolism, since respiration accounted on average for 51% of gross primary production integrated over the euphotic layer.


*Keywords:* Phytoplankton; Primary productivity; Equatorial Atlantic; Upwelling; Atlantic Meridional Transect

## 1. Introduction

The determination of the role of the tropical open ocean in the global carbon cycle has been the objective of intense research during the past decade (e.g. Longhurst, 1993; Murray et al., 1994; Le Borgne et al., 2002). Much of our understanding of the relevant biological processes in these areas derives from studies conducted in the Pacific Ocean, mainly related to its contribution to ocean–atmosphere $CO_2$ fluxes or to its response to the interannual variability forced by the El Niño Southern Oscillation (ENSO) (e.g. Murray et al., 1995; Barber et al., 1996; Chavez et al., 1999). Comparatively, much less attention has been paid to the investigation of biologically mediated carbon cycling in the Equatorial Atlantic.

The Equatorial Atlantic, frequently divided into two different biogeographic provinces (Longhurst, 1998), the Eastern Tropical Atlantic (ETRA) and the Western Tropical Atlantic (WTRA), displays a banded current structure resulting from the trade winds regime. The main westward flows at the surface are the North Equatorial Current (NEC; 10°–15°N) and the South Equatorial Current (SEC; 3°N–15°S), balanced by three eastward currents: the highly seasonal North Equatorial Countercurrent (NECC), located at the surface between 3° and 10°N, the South Equatorial Countercurrent (SECC), also superficial, weak and variable, and the Equatorial Undercurrent (EU), centred at the Equator at ca. 100 m depth (Tomczak and Godfrey, 1994). The different direction of the Ekman transport on both sides of the Equator causes a divergence southwards of the Equator bringing into the surface layer relatively nutrient-rich water from the EU. This results in an enhancement of phytoplankton biomass, which is permanently visible, albeit with seasonally changing intensity, in global maps of surface ocean chlorophyll (e.g. Signorini et al., 1999).

A characteristic feature of the tropical and subtropical Atlantic is the presence of a quasi-permanent "Typical Tropical Structure" (TTS; Herbland and Voituriez, 1979), whereby a nutrient-depleted upper mixed layer is separated from a light-limited lower layer by a strong density gradient. A deep chlorophyll maximum (DCM) typically develops at or near the pycnocline depth (e.g. Agustí and Duarte, 1999). The equatorial upwelling can modify this two-layer structure by introducing nutrients into the euphotic layer and causing a shallowing of the DCM (Herbland et al., 1987; Longhurst, 1993; Monger et al., 1997). Phytoplankton biomass and primary production in the equatorial region show a large degree of variability, with averaged C fixation rates ranging from ~120 to ~1000 mg $C\,m^{-2}\,d^{-1}$ (Minas et al., 1983; Marañón et al., 2000, 2001; Serret et al., 2001). This variability could derive from short-term changes in the current system (Herbland and Le Bouteiller, 1982; Herbland et al., 1983) and also from interannual differences in atmospheric forcing. The relationship between the equatorial upwelling and enhanced rates of primary production seems to be far from simple. Thus, some studies have reported high levels of primary production and phytoplankton biomass associated with the seasonal advection of subsurface nutrient rich waters (e.g. Bauerfeind, 1987). Other studies, however, found no differences in primary production between the strong upwelling and weak upwelling periods (Oudot and Morin, 1987), and Herbland et al. (1987) suggested that the upwelling only produces an upward displacement of the chlorophyll maximum without increasing the production or biomass of phytoplankton. It is also well known that phytoplankton size structure

remains rather constant, dominated by small phytoplankton cells, in spite of the wide range of primary production rates measured in the region (Herbland et al., 1985; Bauerfeind, 1987).

Little is known about other components of the planktonic community in the Equatorial Atlantic. Zubkov et al. (2000, 2000a) measured heterotrophic bacterial abundances and production during two meridional transects in the Atlantic Ocean. Their results in the equatorial region (10°N–10°S) showed up to two-fold variations in bacterial abundances and production rates, probably related to seasonal variability (Zubkov et al., 2000). Measurements of net community production in this region are also scarce and derive from large-spatial-scale studies as well (González et al., 2002; Serret et al., 2001). González et al. (2002) visited the 10°N–10°S region in Spring and Autumn 1997 and found a balanced or net heterotrophic community metabolism. Serret et al. (2001) found a negative production/respiration balance in June 1998 in the same region, but this study was located closer to the African coast and did not include the equatorial divergence. The reduced number of measurements together with their large variability both in time and space are likely to be responsible for the observed differences.

Studies focused on the quantification of the biomass and distribution patterns of specific microbial compartments and/or fluxes between compartments in the Equatorial Atlantic have been conducted over the past decades (see references above). However, to the best of our knowledge, a comprehensive study based on the concurrent measurement of the biomass of, and fluxes between, the main components of the microbial community has not been attempted previously in this oceanic region. The objective of this investigation was to construct a carbon budget for the microbial plankton of the Equatorial Atlantic. With this aim, we concurrently measured size-fractionated phytoplankton Chl-*a* and production together with bacterial biomass and production, and microbial oxygen production and respiration along a latitudinal section crossing the eastern Equatorial Atlantic. This data set, collected in contrasting thermohaline environments, allowed further study of the relationships between nutrient supply, phytoplankton community structure and microbial community metabolism in the open ocean.

## 2. Methods

Fourteen stations were visited in the Equatorial Atlantic Ocean (10°N–10°S) from 24 to 30 September 2000 (Fig. 1) on board RSS James Clark Ross, during the Atlantic Meridional Transect 11 (AMT 11) cruise, as part of a broader research programme (see Aiken et al., 2000). Two stations were sampled daily between 04:00 and 05:00 GMT and between 10:00 and 11:00 GMT. Except for Chl-*a* concentration and bacterial production, which were measured on every station, all chemical and microbiological measurements presented here were carried out on water collected during the early morning stations, which were located at approximately 350 km intervals.

MODIS images of Chl-*a* concentration (mg Chl-*a* $m^{-3}$) in the study region were provided by the NASA/Goddard Space Flight Center for the period 13–28 September 2000. Simultaneous images of sea surface temperature (SST) anomaly (°C; SST minus zonal mean) were elaborated using SST data (NOAA OI SST V2 archive; $1^\circ \times 1^\circ$ resolution) from the NOAA Climate Diagnostic Centre (CDC).

Vertical profiles of photosynthetically active irradiance (PAR, 400–700 nm) were obtained at the late morning stations by integrating measurements of downwelling irradiance at seven SeaWiFS wavelength bands as measured with an optical profiler (SeaOPS) (Aiken et al., 2000). The vertical distribution of temperature and salinity was determined using a Seabird 911 + CTD fitted to a rosette system provided with 12 × 10-l Niskin bottles. Samples for nutrient analysis were collected daily from all sampling depths into 60 ml HDPE (Nalgene) bottles and analysed immediately after collection. Nutrient analyses were carried out using air-segmented-flow, colorimetric analytical techniques with a Technicon Autoanalyzer II. The analytical method used for nitrate was that developed by Brewer and Riley (1965)

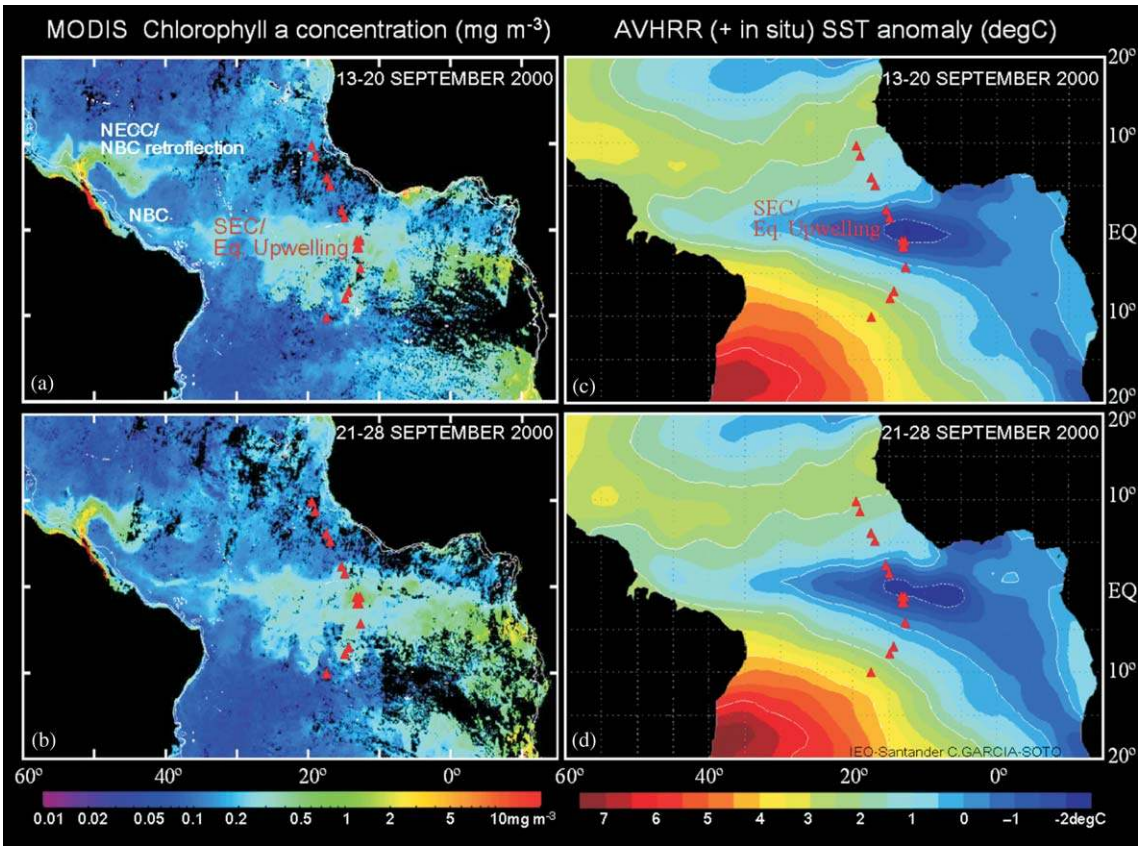


Fig. 1. Location of sampling stations (red triangles) in the Equatorial Atlantic Ocean during the AMT 11 cruise superimposed on MODIS Chl-*a* concentrations (mg Chl-*a* $m^{-3}$) for the period (a) 13–20 September 2000 and (b) 21–28 September 2000, and sea surface temperature (SST) anomaly (deg C; SST minus zonal mean) for the period (c) 13–20 September 2000 and (d) 21–28 September 2000.

and modified for increased sensitivity according to Woodward (1994). Nitrite was measured using the method of Grasshoff (1976) and silicate and phosphate were determined according to Kirkwood (1989).

Dissolved oxygen concentration was measured at 9–10 depths within the upper 250 m. Acid washed, gravimetrically calibrated, 120 ml borosilicate glass bottles were carefully filled from the Niskin bottle using silicon tubing. Fixing and storage procedures, reagents and standardisation followed the recommendations by Grasshoff (1976). Measurements of dissolved oxygen were made with an automated Winkler titration system Metrohm 721 Net Titrino, using a potentiometric end point (Oudot et al., 1988; Pomeroy et al., 1994). Aliquots of fixed samples were delivered with a 50 ml overflow pipette. Oxygen saturation was calculated using the equations for oxygen solubility in seawater of Benson and Krause (1984).

At every station, samples were collected from 5 to 7 depths in the upper 200 m. Water samples (200–300 ml) were sequentially filtered through 20, 2 and 0.2 μm pore size polycarbonate filters of 47 mm diameter (Poretics PC, Millipore GTTP and Millipore TTTP, respectively). Chl-*a* was extracted in 90% acetone at –20°C for about 24 h. Samples were analysed using a Turner 10-AU fluorometer calibrated with pure Chl-*a* standards. Total Chl-*a* was determined from the addition of size fractionated measurements. Chemically deter-

mined Chl-*a* values were used to calibrate the CTD fluorometer (Chl-$a = 0.67$ Fluorescence—0.7, $n = 211$, $r^2 = 0.83$, $p < 0.001$). Phytoplankton biomass (Phyto C) was estimated from vertically integrated Chl-*a* measurements by assuming an overall C:Chl-*a* ratio of 80 for the whole photic layer (e.g. Campbell et al., 1994; Taylor et al., 1997).

Polyethylene bottles (250 ml) containing 1.25 ml Lugol's solution acidified with acetic acid were filled with seawater from the same depths as for $^{14}C$ incorporation experiments. Identification and counting of nano and microplankton were carried out with an inverted microscope on 50 ml composite sedimentation chambers.

For the determination of primary production, seawater samples were collected from five depths down to a depth determined from the vertical distribution of temperature and fluorescence, together with the record of the vertical PAR profiles obtained at the previous late morning station. These depths were chosen to correspond to optical depths ranging from 97% to 1% of surface irradiance. Immediately after collection, water samples from each depth were transferred to four 75 ml acid-cleaned polystyrene bottles (3 light and 1 dark), inoculated with 370–740 kBq (10–20 μCi) $NaH^{14}CO_3$ and incubated for 24 h. Before dawn, samples were placed in an on-deck incubator that simulated the irradiance at the original sampling depths by means of various combinations of neutral density and blue plastic filters. Samples were refrigerated with running seawater pumped from a depth of seven meters. During the night, incubators were covered with opaque bags in order to avoid artefacts due to the ship's deck lights. After the incubation period, samples were sequentially filtered through 20, 2, and 0.2 μm polycarbonate filters at very low vacuum pressure (<50 mmHg). Decontamination of the filters was achieved by exposing them to concentrated hydrochloric acid (HCl) fumes for 12 h. After decontamination, the filters were transferred to scintillation vials to which 4 ml of scintillation cocktail (Ultima Gold, Packard) were added. Radioactivity in each sample was measured on a Beckman LS6000 SC scintillation counter. Quenching was corrected using an external standard. Dark bottle values were subtracted from the counts obtained in the light samples. Total primary production was determined by adding the size fractionated rates.

Abundance of coccoid cyanobacteria and heterotrophic bacteria was determined in samples preserved with glutaraldehyde (5% final concentration) following the method of Porter and Feig (1980). Ten millilitre of each sample were filtered onto 0.2 μm black polycarbonate membrane filters and stained with DAPI (4′-6-diamidino-2-phenylindole) for 5 min. The filters were mounted using low-fluorescence oil onto microscope slides and stored frozen. Bacteria were counted using ultraviolet light with an epifluorescence microscope (Olympus BH-2). Cyanobacteria were counted on the same slides observed under blue light and were distinguished from heterotrophic bacteria by their emission of yellow-orange autofluorescence. We estimate that ca. 20% of heterotrophic bacterial numbers obtained during AMT 11 were likely *Prochlorococcus* cells. The low Chl-*a* content and loss of fluorescence after fixation make these cells difficult to identify on DAPI stained samples. Bacterial cellular carbon content was estimated from biovolumes using the empirical equation of Norland et al. (1987) for bacteria ranging from 0.001 to 0.5 $\mu m^3$: $C = 0.09\ BV^{0.9}$ where C is the carbon content (pg C $cell^{-1}$) and BV is the bacterial biovolume ($\mu m^3\ cell^{-1}$). Bacterial biovolumes were computed from measurements of bacterial dimensions using a graduated bar coupled to the microscope eyepiece. Cocci were considered as spheres and rods as cylinders.

Production of heterotrophic bacteria was estimated by $^3H$-leucine incorporation, using the method described by Kirchman (1993) but replacing the final filtration step by centrifugation (Smith and Azam, 1992). Four 1 ml aliquots of water samples collected from each depth were inoculated with $^3H$-leucine to a final concentration of 50 nM and incubated for 30 min in 1.5 ml Eppendorf vials at surface temperature. In addition, two 1 ml controls killed with trichloroacetic acid (TCA, 5% w/v final concentration) were incubated for each depth. Incubations were terminated by the addition of 5% TCA to the incubation vials. Dissolved leucine was removed from the incubation vials by repeated washing

with 5% TCA and successive centrifugation (12,000 r.p.m., 10 min). Scintillation cocktail (Ultima X-Gold, Packard) was added to the vials and radioactivity measured in a liquid scintillation counter (LKB Wallac). The conversion factors between leucine incorporation and carbon production were estimated in on board experiments, following the procedures of Bjørnsen and Kuparinen (1991) and Kirchman and Ducklow (1993). For each experiment, 200 ml of surface water were diluted in 1000 ml of 0.2 μm filtered seawater and incubated at room temperature (~20 °C) for 32 h. Every 4 h, aliquots of this culture were removed for the determination of bacterial abundance and leucine incorporation rates by the described procedures. The factor used for this study was 0.73 kg C mol Leu$^{-1}$, the average (SD = 0.25) of two experiments carried out with surface water during AMT 11 and another experiment carried out during cruise CIRCANA-1 (autumn 2001, Morán et al., 2004), all performed at oligotrophic stations.

Gross primary production (GPP), net community production (NCP) and dark community respiration (DCR) were determined at five depths from in vitro changes in dissolved oxygen after light and dark bottle incubations. Sampling and incubation were carried out at the same depths, simultaneously and under the same conditions as for $^{14}$C incorporation experiments. Twelve 120 ml, gravimetrically calibrated, acid washed borosilicate glass bottles were carefully filled from each Niskin bottle by means of a silicone tube, overflowing by >250 ml. Care was taken to minimise exposure of the samples to light or temperature changes during sampling from Niskin bottles. From each depth, four replicate bottles were fixed immediately for initial oxygen concentrations, four bottles were kept in darkness and four bottles incubated under irradiance conditions simulating those of the original sampling depth as described above. After the 24 h incubation period, dissolved oxygen concentration was determined following the method described above. Production and respiration rates were calculated from the difference between the means of the replicate light and dark incubated and zero time analyses: NCP = measured $\Delta O_2$ in light bottles (mean of $[O_2]$ in 24 h light−mean initial $[O_2]$); DCR = measured $\Delta O_2$ in dark bottles (mean initial $[O_2]$−mean $[O_2]$ in 24 h dark); GPP = NCP + DCR.

We calculated gross carbon photosynthesis from gross $O_2$ production, assuming a photosynthetic quotient (PQ) of 1.2 and a respiratory quotient (RQ) of 1.1 (Bender et al., 1999). Relative contribution of different size-classes to gross carbon production was assumed to be equivalent to the relative contribution of the different size-classes to the measured $^{14}$C incorporation rate.

Euphotic zone integrated values of size fractionated and total Chl-*a*, particulate carbon production (POC), GPP, DCR and NCP were obtained by trapezoidal integration of the volumetric data down to the depth of 1% surface incident irradiance. Euphotic zone depth ranged from 55 m in the equatorial upwelling area to 100 m near 10°S.

## 3. Results

### 3.1. Remote sensing data

Relatively high MODIS Chl-*a* concentrations (≥0.5 mg Chl-*a* m$^{-3}$) were found associated with cold surface waters (SST anomalies ca. −2.5°C) at the equatorial region during the period 21–28 September, when in situ measurements were carried out (Fig. 1). SST increased progressively whereas Chl-*a* concentration decreased towards the subtropical gyres. The magnitude and distribution patterns of SST anomaly and Chl-*a* concentration did not differ notably from those obtained one week before (13–20 September) (Fig. 1). Examination of daily maps of Chl-*a* concentration from 13 to 28 September (Fig. 2) showed a persistent band of relatively high Chl-*a* values centred near the Equator. The low daily variability found during this period of the year suggests that weekly averaged Chl-*a* concentrations (Fig. 1) are representative of the cruise period.

### 3.2. Hydrography

The latitudinal distribution of thermohaline properties during the AMT 11 cruise (Fig. 3)

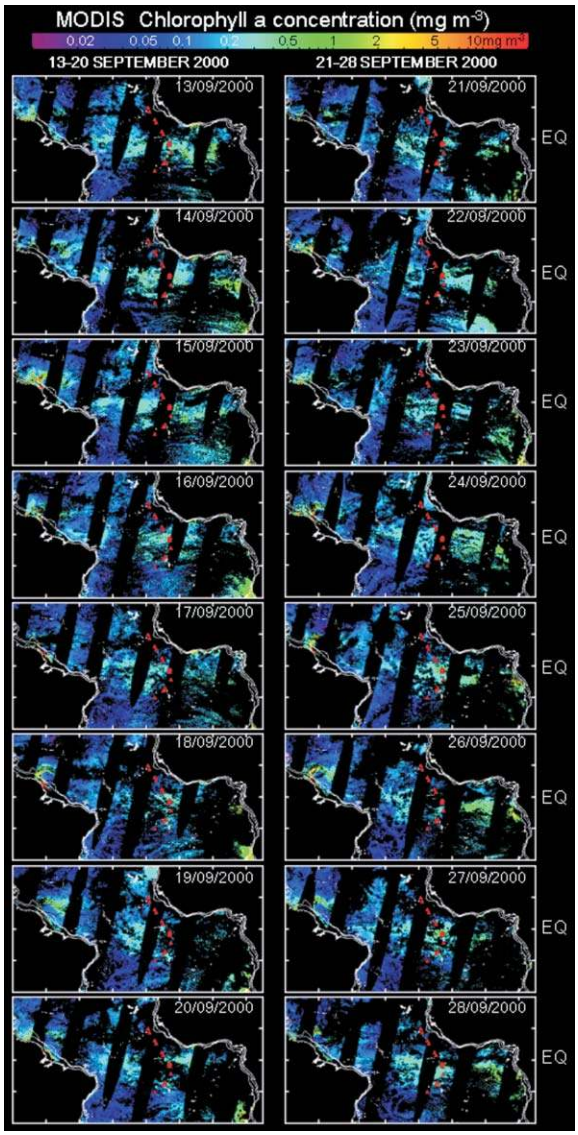


Fig. 2. Daily images of MODIS Chl-*a* concentration (mg Chl-*a* $m^{-3}$) from 13 to 28 September 2000.

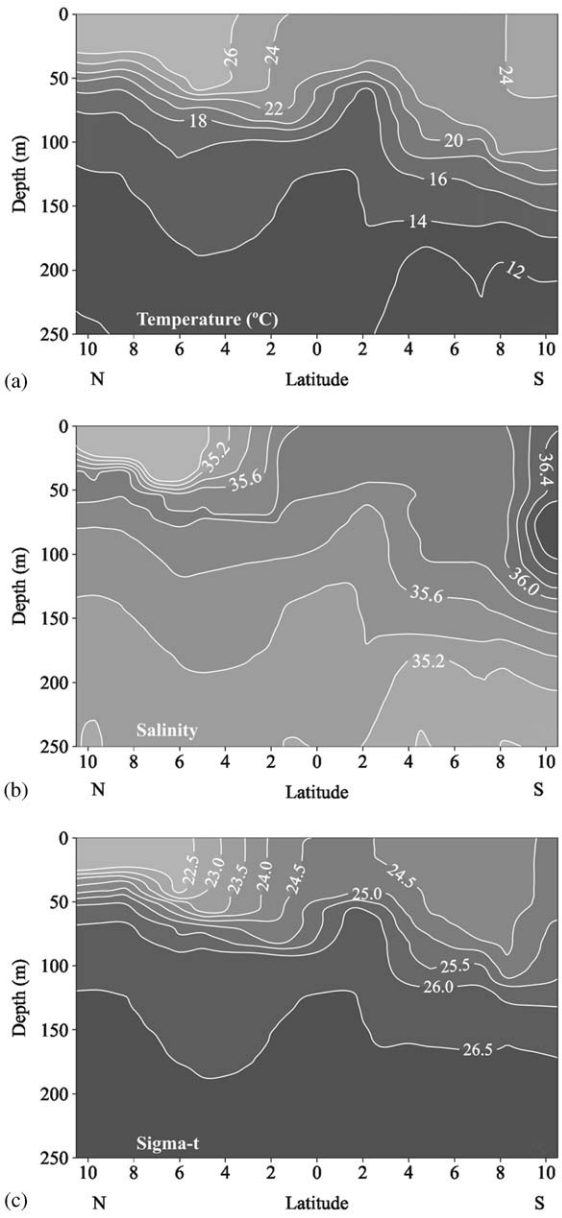


Fig. 3. Vertical distribution of (a) temperature (°C), (b) salinity and (c) sigma-*t* from 10°N to 10°S during the AMT 11 cruise.

reflected the physical characteristics of the Eastern Tropical Atlantic province (ETRA; Longhurst, 1998). The thermocline was located at about 50 m in the northernmost part of the section (10°N), its position deepened progressively southward until 4°N, where it reached 75 m at the North Equatorial Countercurrent (NECC) (Fig. 3a). Above it, a warm (>26 °C), low salinity (<35.2) mixed layer was found (Fig. 3b). Sigma-*t* distribution (Fig. 3c) showed a low-density (<22.5) upper layer in the northernmost part of the section. Uplifting of isopycnals indicated the location of the equatorial divergence at 2°S, where the thermocline was at

50 m depth. Thermocline shallowing in this area (from 1°N to 4°S) led to minimum SST (<24 °C). Salinity maximum reached the surface between 2°N and 8°S. From 8°S southward, SST increased progressively as the thermocline and halocline deepened and the cruise track approached the South Atlantic Gyral province (SATL; Longhurst, 1998). In this region, salinity increased abruptly reflecting a frontal system associated with the transition from the ETRA to the SATL province.

### 3.3. Nutrients and oxygen concentration

The northernmost part of the studied area was characterised by a nitrate-depleted upper layer (nitrate levels <0.1 μM) separated from a deeper, nitrate-rich layer (>20 μM) by a strong gradient located at the depth of the thermocline (Fig. 4a). The highest surface nitrate concentrations (>1 μM) were measured in the equatorial divergence area (2°N–5°S), where the nitracline shoaled to the surface. This nitrate enrichment was accompanied by relatively high surface levels of phosphate (>0.2 μM) and silicate (>1.5 μM) (data not shown). From 7°S southward, nitrate levels below the detection limit of the autoanalyser (25 nM) were found in the mixed layer as the nitracline deepened near the SATL province, reaching 75 m depth.

Relatively high levels of $O_2$ saturation (% $O_2$ sat >102%) were observed near the surface northward of the equatorial upwelling (Fig. 4b). At the equatorial divergence, the upwelling of deep and nutrient rich water was associated with a decrease of $O_2$ saturation in subsurface waters, however the %$O_2$ sat remained >100 at the surface. From 7°S to the SATL province $O_2$ saturation values close to 100% extended from the surface to 70 m.

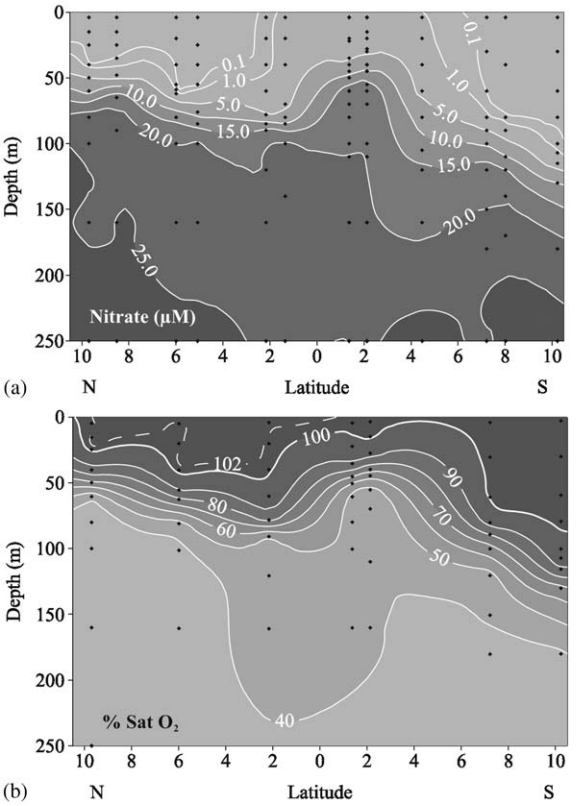


Fig. 4. Vertical distribution of (a) $NO_3^-$ concentration (μM) and (b) percentage of oxygen saturation from 10°N to 10°S during the AMT 11 cruise.

### 3.4. Chl-a concentration and phytoplankton composition

In the northern part of the section, a deep Chl-*a* maximum (DCM) (>0.3 mg Chl-*a* $m^{-3}$) was found at the level of the thermocline, near the bottom of the euphotic layer (Fig. 5a). Low Chl-*a* concentrations (<0.2 mg Chl-*a* $m^{-3}$) were measured in the nutrient depleted upper layer. From 3°N to 3°S, relatively high Chl-*a* concentrations were measured in surface waters. The surface Chl-*a* maximum (>0.5 mg Chl-*a* $m^{-3}$) was centred at 1.5°S and extended vertically down to 40 m depth. As the cruise track approached the SATL province, surface Chl-*a* concentrations decreased (<0.2 mg Chl-*a* $m^{-3}$) and the DCM deepened to 110 m at 10.5°S. Photic depth integrated Chl-*a* concentration ranged from 14 mg Chl-*a* $m^{-2}$ at 10°S to 30 mg Chl-*a* $m^{-2}$ at 7°S, averaging (±SE) 22±1 mg Chl-*a* $m^{-2}$ in all the studied area.

The contribution of picoplankton (<2 μm cells) to total Chl-*a* always exceeded 45% (Fig. 5b). The lowest contribution of picoplankton to total Chl-*a* was found in the equatorial divergence, whereas in the rest of the section phytoplankton <2 μm

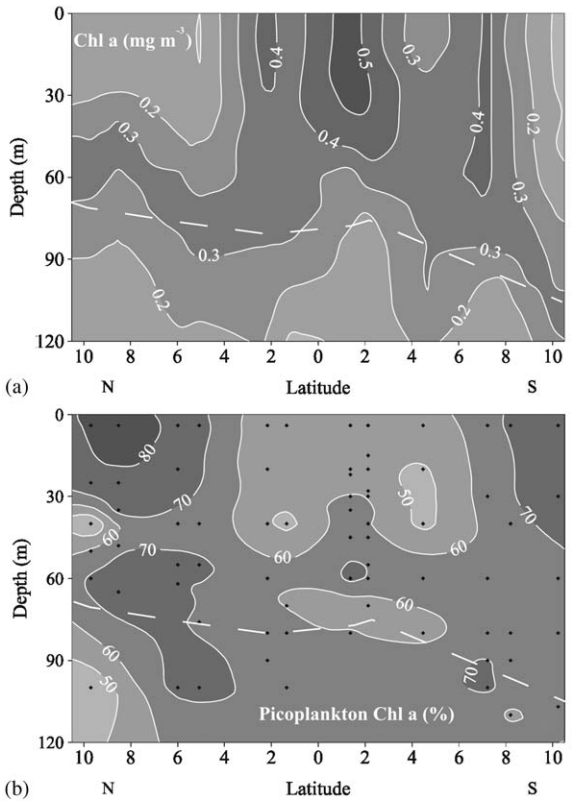


Fig. 5. Vertical distribution of (a) chlorophyll-*a* (mg Chl-*a* $m^{-3}$) and (b) relative contribution of $<2\,\mu m$ phytoplankton to total chlorophyll-*a* (%) from 10°N to 10°S during the AMT 11 cruise. The dashed line indicates the depth corresponding to 1% surface irradiance.

represented >60% of total Chl-*a*. Photic depth integrated contribution of picoplankton to total Chl-*a* concentration ranged from 53% to 74% with an averaged value of 64±2%. No significant relationship was found between the relative contribution of picoplankton and total Chl-*a* concentration.

The community of photoautotrophs was numerically dominated by cyanobacteria and dinoflagellates. Different groups of microbial plankton showed contrasting latitudinal and vertical distribution patterns (Fig. 6). Small ($<30\,\mu m$) pennate and centric diatoms together with *Pseudonitzschia* spp. and *Nitzschia* spp. formed the bulk of diatoms. Higher abundances of diatoms, flagellates (8–10 μm monads) and cryptophyta (*Cryptomonas* spp.) were found in surface waters, close to the equatorial divergence. *Heterocapsa niei, Torodinium robustum, Oxytoxum coronatum* and unidentified $<30\,\mu m$ cells were the most abundant dinoflagellates. Dinoflagellates showed their highest surface abundances on both sides of the equatorial divergence. Relatively high numbers of flagellates, dinoflagellates and cryptophyta were found at the DCM. Protozoa, dominated by ciliates, reached higher values at 40 m depth in the equatorial divergence and over the DCM at 10°N. The highest abundances of cyanobacteria were found in surface waters, particularly in the equatorial divergence area.

### 3.5. Primary production

The latitudinal distribution of primary production rates (Fig. 7a) mirrored those of Chl-*a* except in the southern part of the region. Low C incorporation rates ($<8$ mg C $m^{-3}$ $d^{-1}$) were observed in surface waters from 10°N to 5°N. In this region, primary production increased with depth, reaching a maximum value at about 50 m depth, coinciding with the DCM. The highest surface primary production rates ($>28$ mg C $m^{-3}$ $d^{-1}$) occurred at the Equator. C fixation rates decreased gradually from 1°S to 10°S in the whole upper mixed layer. Integrated primary production in the euphotic layer varied between 218 and 1337 mg C $m^{-2}$ $d^{-1}$. The highest values were found in the equatorial upwelling and the lowest in the southern part of the study area. The mean value calculated for the region was $680 \pm 141$ mg C $m^{-2}$ $d^{-1}$.

As with Chl-*a*, the relative contribution of picoplankton to C fixation (Fig. 7b) was always higher than 45%. The highest percentages were associated with the NECC. High values were also observed below the thermocline. The relative contribution of picoplankton to total primary production was lower near the equatorial upwelling. Low contributions were also observed in the euphotic layer to the south of the equatorial divergence contrasting with the distribution of Chl-*a* $<2\,\mu m$. Photic depth integrated contributions of picoplankton to total primary production

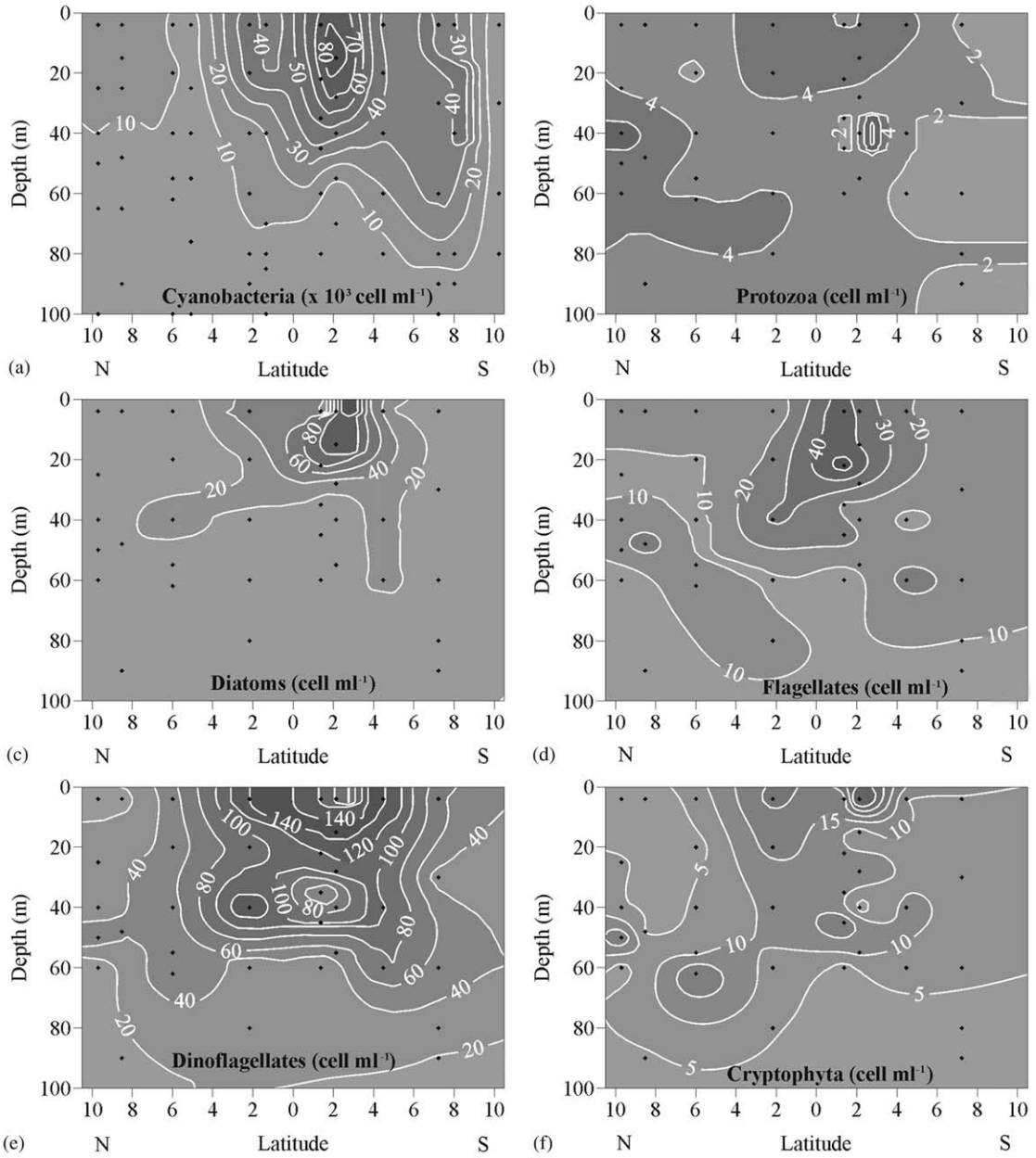


Fig. 6. Vertical distribution of the cell abundance (cell $ml^{-1}$) of (a) cyanobacteria ($\times 10^3$ cell $ml^{-1}$), (b) protozoa, (c) diatoms, (d) flagellates, (e) dinoflagellates and (f) cryptophyceae from 10°N to 10°S during the AMT 11 cruise.

ranged from 54% to 72%, measured respectively to the south and to the north of the equatorial divergence, with an average value of $60 \pm 2\%$.

### 3.6. Bacterial abundance and production

The vertical distribution of bacterial abundance (Fig. 8a) showed a surface maximum

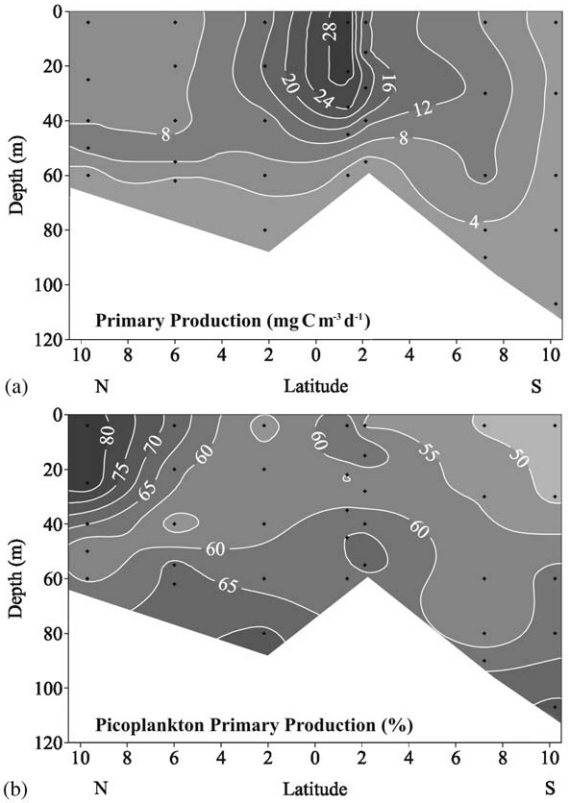


Fig. 7. Vertical distribution of (a) primary production rate (mg $C\,m^{-3}\,d^{-1}$) and relative contribution of $<2\,\mu m$ phytoplankton to total primary production (%) from 10°N to 10°S during the AMT 11 cruise.

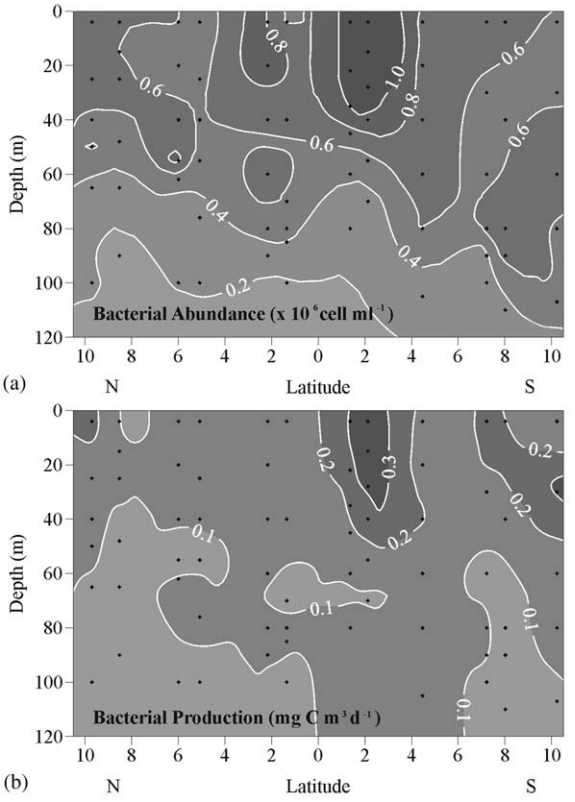


Fig. 8. Vertical distribution of (a) bacterial abundance ($\times 10^6$ cell $ml^{-1}$) and (b) bacterial production (mg $C\,m^{-3}\,d^{-1}$) from 10°N to 10°S during the AMT 11 cruise.

($6 \times 10^5$ cell $ml^{-1}$) down to 40 m depth between 10°N and 8°N. This maximum deepened following the DCM, reaching 55 m depth at 6°N. The highest bacterial abundances ($>10^6$ cell $ml^{-1}$) were found in the upper 40 m of the equatorial divergence area. From the equatorial divergence southwards, surface bacterial abundances decreased and a subsurface maximum was observed. Photic zone integrated bacterial abundances ranged from $36 \times 10^{12}$ cell $m^{-2}$, measured in the northern part of the studied area, to $74 \times 10^{12}$ cell $m^{-2}$, measured in the equatorial divergence. The mean bacterial abundance for the Equatorial Atlantic estimated in this study was $53 \pm 3 \times 10^{12}$ cell $m^{-2}$.

Bacterial production rates in the photic zone generally exceeded 0.1 mg $C\,m^{-3}\,d^{-1}$ (Fig. 8b). Maximum rates ($>0.3$ mg $C\,m^{-3}\,d^{-1}$) occurred in the upper 30 m of the equatorial divergence and in subsurface waters at 10°S (Fig. 8b). Rates of 0.2 mg $C\,m^{-3}\,d^{-1}$ were found in surface waters at 10°N and 7°S–8°S. Photic zone integrated bacterial production ranged from 5 to 28 mg $C\,m^{-2}\,d^{-1}$. The lowest photic zone integrated rates were measured at 8°N and the highest rates at the equatorial divergence. The resulting mean for the equatorial region was $12 \pm 2$ mg $C\,m^{-2}\,d^{-1}$.

### 3.7. Oxygen fluxes

The highest values of dark community respiration (DCR) ($>2$ mmol $m^{-3}\,d^{-1}$) were found in subsurface waters (at about 40–50 m depth) of the equatorial upwelling, underneath the high primary

production layer where Chl-*a* concentration was also relatively high (Fig. 9a). DCR rates showed relatively high values throughout the water column in the equatorial divergence region and in surface waters of the northernmost part of the section. At the rest of the stations, DCR did not show large vertical variability. Photic zone integrated DCR rates ranged from 46 to 99 mmol $O_2\,m^{-2}\,d^{-1}$ with higher rates located in the equatorial divergence area. The averaged integrated DCR rate for the Equatorial Atlantic estimated in this study was $71 \pm 7$ mmol $O_2\,m^{-2}\,d^{-1}$.

Net community production (NCP) distribution (Fig. 9b) exhibited a marked vertical gradient. High positive rates were measured throughout the mixed layer in the equatorial divergence. Negative values were measured in the upper meters of the water column at 10°N and 10°S and below the thermocline from 10°N to 10°S. Depth integrated NCP rates ranged from 39 to 124 mmol $O_2\,m^{-2}\,d^{-1}$ with higher rates at the equatorial divergence and averaged $80 \pm 18$ mmol $O_2\,m^{-2}\,d^{-1}$ for the entire region.

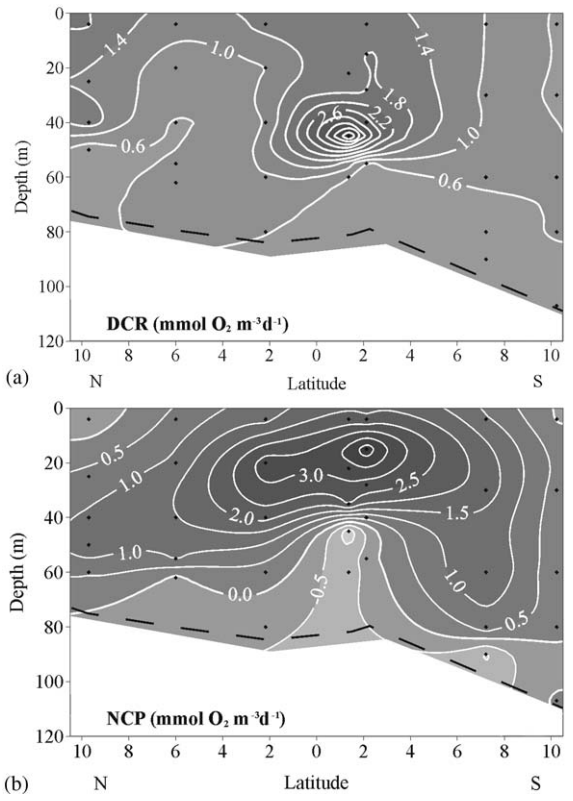


Fig. 9. Vertical distribution of (a) dark $O_2$ community respiration (DCR) and (b) net community production (NCP), both in mmol $O_2\,m^{-3}\,d^{-1}$. The black dashed line indicates the depth corresponding to 1% surface irradiance.

### 3.8. Carbon budget

The concurrent determination of the biomass of different microbial groups together with the fluxes of production and respiration allowed us to construct the carbon budget for the euphotic layer of the Equatorial Atlantic Ocean area studied here (Fig. 10a). Gross primary production was high ($1517 \pm 230$ mg C $m^{-2}\,d^{-1}$). Picophytoplankton dominated (>60% contribution) both primary production and phytoplankton biomass. Bacterial biomass ($582 \pm 34$ mg C $m^{-2}\,d^{-1}$) represented about one-third of the estimated phytoplankton carbon. However, bacterial production amounted to only 0.9% of total primary production and the net community metabolism was autotrophic (only about 50% of the organic carbon produced photosynthetically was consumed by the microbial community).

In order to compare the microbially mediated fluxes in two contrasting hydrographic regimes, carbon budgets were also built up separately for the region characterised by the TTS (10°N–2°N and 9°S–10°S, Fig. 10b), where a nitrate-depleted, low Chl-*a* upper mixed layer was found (see Figs. 4a and 5a), and for the equatorial upwelling region (2°N–5°S, Fig. 10c) characterized by a nitrate-rich upper mixed layer where $NO_3^-$ concentrations were $\geqslant 0.4\,\mu M$ (see Figs. 4a and 5a). Gross primary production in the equatorial upwelling was double that of the TTS region. However, the contribution of picoplankton to total primary production in both regions did not show large variations. Phytoplankton biomass was significantly higher (*t*-test, $p<0.05$, $n=12$) in the equatorial upwelling. Picophytoplankton C remained nearly constant and dominated phytoplankton biomass in all the study area, although a significant increase (*t*-test, $p<0.001$, $n=12$) in the relative contribution of >2 μm phytoplankton to total phytoplankton C was found in the upwelling region. Differences

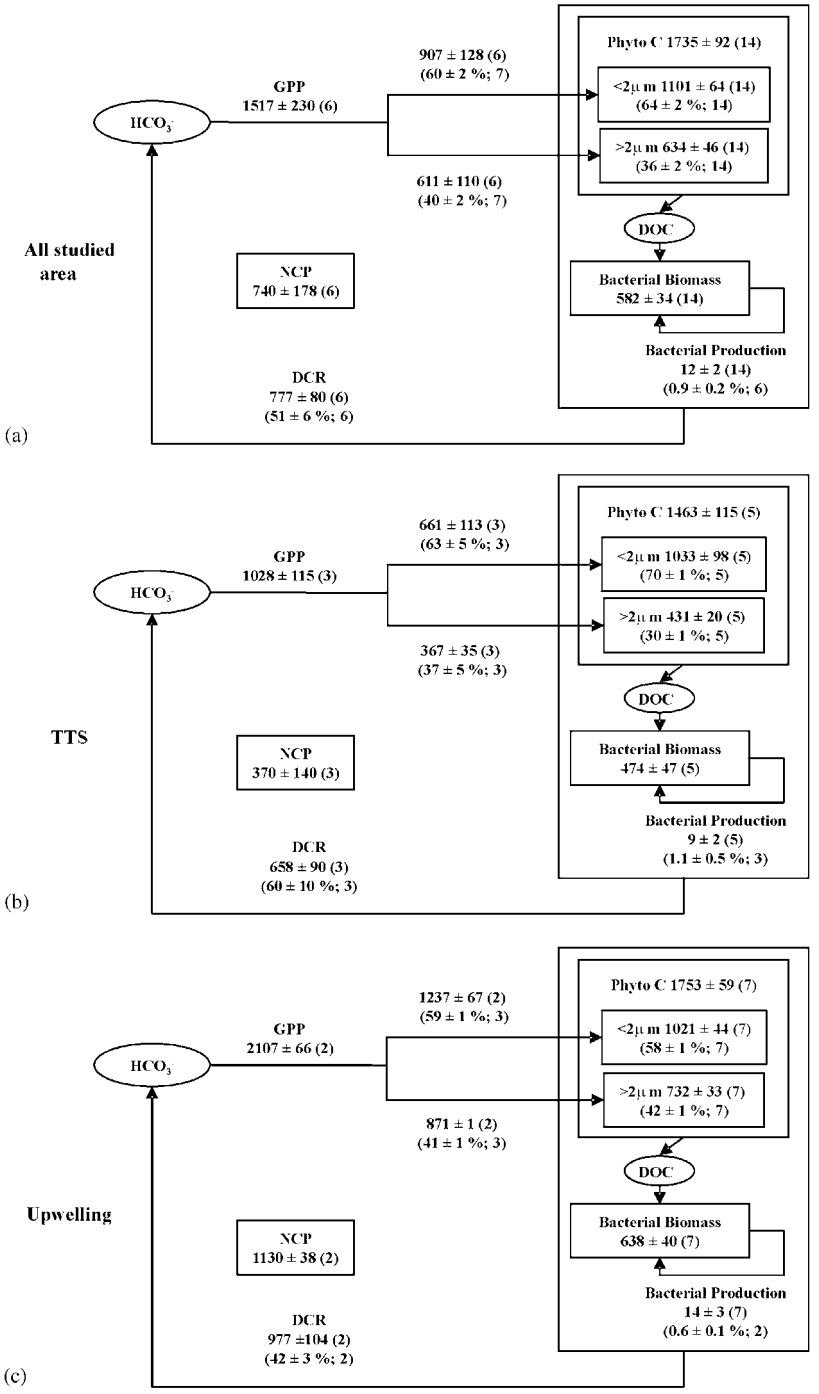


Fig. 10. Carbon budget for (a) the whole study area during the AMT 11 cruise (10°N–10°S), (b) typical tropical structure (TTS) stations (10°N–2°N and 9°S–10°S), and (c) upwelling stations (2°N–5°S). Biomass is expressed in mg $C\,m^{-2}$ ($\pm$ SE). Fluxes are expressed in mg $C\,m^{-2}\,d^{-1}$ ($\pm$ SE). Numbers in parentheses represent the relative contribution of any given flux or phytoplankton size class with respect to gross primary production (GPP) or total phytoplankton biomass, respectively, followed by the number of observations. DCR: dark community respiration; NCP: net community production; DOC: dissolved organic carbon. See the 'Methods' section for details on calculations and conversion factors.

in bacterial production between both regions were not significant despite the significantly (*t*-test, $p<0.05$, $n=12$) higher bacterial biomass found in the upwelling area. Respiration rates were not statistically different between the two regions. Net microbial community metabolism was autotrophic both in the equatorial upwelling and in the TTS region although, the percentage of primary production respired by the microplanktonic community was higher in the TTS region.

## 4. Discussion

### *4.1. Phytoplankton size structure and primary production*

The photic layer of the Equatorial Atlantic region investigated in this study was characterized by relatively high photosynthetic carbon incorporation rates. The values of integrated primary production measured in the Equatorial Atlantic (from 2°N to 5°S) during our study (average ±SE: $995 \pm 171$ mg C m$^{-2}$ d$^{-1}$) agree with previous data obtained during autumn and winter, which averaged: $847 \pm 81$ mg C m$^{-2}$ d$^{-1}$ (ranged from 92 to 1660 mg C m$^{-2}$ d$^{-1}$, $n=33$; Minas et al., 1983; Marañón et al., 2000, 2001; Serret et al., 2001). The enhanced productivity measured in the divergence region was closely related to the increase in surface nitrate concentration resulting from the equatorial upwelling. The observation of higher surface nitrate concentrations during the upwelling intensification period (usually from June to October) has been recurrent in earlier studies (Minas et al., 1983; Oudot,1983; Bauerfeind, 1987; Oudot and Morin, 1987).

We observed two distinct ecological situations in the Equatorial Atlantic: the typical tropical structure (TTS) from 10°N to 2°N and in the southern end of the transect, close to the SATL province and the equatorial divergence area (ca. 2°N–5°S), characterized by different vertical distributions of nutrients, Chl-*a* and primary production. In the equatorial upwelling area, the presence of nitrate in surface waters led to enhanced photic layer integrated rates of primary production which translated also into a moderate but significant increase in the biomass of phytoplankton. Picophytoplankton (<2 μm cells) dominated both phytoplankton biomass and production (relative contributions of $64 \pm 2$% of Chl-*a* concentration and $60 \pm 2$% of $^{14}$C-derived primary production, respectively) throughout the area of study (10°N–10°S). The variability in the size-fractionated contribution to total Chl-*a* between the equatorial divergence and TTS stations was relatively minor, despite marked differences in the nitrate concentration throughout the water column; however the highest contribution of <2 μm phytoplankton was found in the upper nutrient-depleted waters away from the divergence, and the lowest (always >45%) was measured in the surface nitrate-rich waters found between 2°N and 5°S. Picophytoplankton contribution to total C incorporation rates showed analogous patterns except south of the equator where the upper, nutrient depleted layer presented the lowest values. A similar dominance of picophytoplankton biomass has been previously reported for the Equatorial Atlantic belt and for the Western Tropical Pacific (Herbland et al., 1985; Le Bouteiller et al., 1992; Zubkov et al., 1998; Marañón et al., 2000). The dominance of small-sized phytoplankton in oligotrophic waters has been frequently explained as a result of the relative advantage of small cells for nutrient uptake (e.g. Raven, 1998). However, recent empirical and experimental studies in the oligotrophic areas of the N and S Atlantic subtropical gyres outside the equatorial region found that the relative contribution of >2 μm phytoplankton to total primary production was consistently greater than their contribution to total Chl-*a* (Fernández et al., 2003).

During the AMT 11 cruise picophytoplankton dominated in both the oligotrophic TTS waters and also in surface waters of the equatorial divergence, where relatively high nitrate concentrations were found. In this situation, a higher contribution of large cells to total Chl-*a* would have been expected. Dominance of large sized phytoplankton in eutrophic waters has been attributed to the relaxation of predation pressure that results from the shorter generation time of large phytoplankton cells as compared to their

main predators, the mesozooplankton. This difference in generation time causes a time lag between microalgal growth and the peak of grazing activity, thus allowing the accumulation of large phytoplankton (Kiorbøe, 1993; Riegman et al., 1993). Our results, however, suggest that this mechanism is not operative in the Equatorial Atlantic.

We found relatively low SST values in the equatorial divergence both during the sampling period and the week before (Figs. 1c and d), which suggests that the intensification of the equatorial upwelling started at least 1 week before the samples were taken. Similarly, ocean colour-derived Chl-*a* concentrations did not show significant daily variations in either magnitude or spatial distribution (Fig. 2). It could be hypothesized that a continuous supply of new nutrients from subsurface layers into the photic zone at the equatorial divergence could favour a close coupling between large phytoplankton cells and mesozooplankton organisms, preventing the outburst of large phytoplankton. In this connection, a positive relationship between phytoplankton and mesozooplankton biomass (measured as dry weight) was found in the Equatorial Atlantic by Le Borgne (1981). During the AMT 11 cruise, Isla et al. (2004) measured mesozooplankton biomass up to 3 g C $m^{-2}$ between 10°N and 10°S and mesozooplankton ingestion rates that removed from 3% to 8% of >2 μm Chl-*a* and from 25% to 33% of >2 μm primary production. Furthermore, Huskin et al. (2001) reported that mesozooplankton grazing in the Equatorial Atlantic region can be responsible for the removal of up to ca. 100% of the primary production and ca. 25–30% of the Chl-*a* stock, although subject to a very high temporal and spatial variability. Such a trophic relevance of mesozooplankton in the Equatorial Atlantic would imply that the confinement of microplankton communities in incubation bottles could result in an overestimation of the contribution of >2 μm phytoplankton to total primary production. Exclusion of mesozooplankton, which mainly grazes on both large phytoplankton and microzooplankton (Harrison and Harris, 1986), would increase the primary production due to large phytoplankton while that due to small sized cells would remain relatively unaffected. Even in this situation, favourable to large phytoplankton cells, we measured contributions of picophytoplankton to primary production higher than those of >2 μm cells, suggesting that other factors beyond predation may be influencing the phytoplankton size-structure.

We cannot rule out nutrient limitation of large phytoplankton cells as an alternative explanation to our observations. In this regard, moderately high nitrate concentrations, together with high nitrate uptake rates (up to 40 nmol $l^{-1}$ $h^{-1}$; Varela et al., submitted), were measured in this study in surface waters of the equatorial divergence, which suggests that a strong nitrate limitation of primary production was unlikely. However, silicate has also been cited as a key controlling factor of both total productivity and phytoplankton size structure in equatorial regions (Dugdale and Wilkerson, 1998). The silicate concentrations measured in this study, ranging between 1.5 and 2.5 μM in the equatorial divergence, are close to the half saturation constants reported for diatoms (0.75–7.5 μM; Leynaert et al., 2001; Ragueneau et al., 2002; Franck et al., 2003) and therefore, silicate limitation of larger diatoms could also at least partially explain the dominance of smaller phytoplankton.

### 4.2. C fluxes and net community metabolism

Carbon and oxygen fluxes measured in the present study are subject to a source of error related to the possible impact of incubation temperature on the rates of $^{14}C$ primary production, oxygen evolution, and bacterial production. In 29% of the samples (10 out of the 35 sampled depths), the difference between in situ and incubation temperature was >2 °C, which could bias the rate estimates. We attempted to correct bacterial production rates using a coefficient ($Q_{10}$) relating temperature increases with bacterial leucine incorporation following the equation $\text{Leu (in situ)} = \text{Leu (incubation)} \times Q_{10}^{0.1*[T(\text{in situ})-T(\text{incubation})]}$, where Leu (in situ) and Leu (incubation) are the leucine incorporation rates in situ and estimated during the incubation, and $T$ (in situ) and $T$ (incubation) are tempera-

tures measured in situ and during the incubation. We chose a $Q_{10}$ value of 2, widely used in plankton studies (Eppley, 1972). This correction yielded values quite similar to the empirical calibration obtained by Zubkov et al. (2000) for a previous AMT cruise: corrected bacterial production rates in the studied area were, on average, $14.2 \pm 6.6\%$ lower than uncorrected values. The effect of temperature on respiration and primary production as measured by the $O_2$ technique is difficult to evaluate, as in this case, there are no empirical relationships which allow the correction of our measurements. However, given that temperature changes tend to have a stronger effect on respiration than on photosynthesis (Lefèvre et al., 1994), the temperature increase experienced by the deep samples during our incubations was likely to lead to an underestimation of the magnitude of the net autotrophic metabolic balance.

In order to build carbon budgets for the region, our results of gross primary production and respiration rates, estimated by the $\Delta O_2$ method, must be converted to C units by means of photosynthetic and respiratory quotients (PQ and RQ, respectively). During this study we measured primary production simultaneously by $^{14}C$ incorporation and by $O_2$ production. Although different processes are involved in the measurement of primary production by the two methods (Bender et al., 1999; Laws et al., 2000; Robinson et al., 2002), we found a good relationship between primary production rates estimated from the $^{14}C$ incorporation and the $O_2$ production method (in both cases derived from 24 h incubations). The empirical relationship obtained between the two photic zone integrated rates was GPP (mmol $O_2\,m^{-2}\,d^{-1}$) $= 2.62$ $PO^{14}CP$ (mmol $C\,m^{-2}\,d^{-1}$) $+ 28.06$, $r^2 = 0.99$, $n = 6$, $p < 0.0001$, which supports our use of a single PQ value for all the studied region. It is worth noting that the slope of this equation does not give the real PQ value but an overestimation, as 24 h $PO^{14}CP$ is possibly closer to net than gross primary production and does not include dissolved organic carbon production, while $\Delta O_2$ GPP measures the rate of photosynthetic activity independently of the fate of the organic matter produced. We converted our $O_2$ fluxes into C fluxes by assuming a PQ of 1.2 and a RQ of 1.1, in accordance with the assumptions of Bender et al. (1999) in the Equatorial Pacific. The use of these quotients yield a $PO^{14}CP$ (mmol $C\,m^{-2}\,d^{-1}$):GPP (mmol $C\,m^{-2}\,d^{-1}$) molar ratio of 0.45, which exactly coincides with the value calculated by Bender et al. (1999) and Laws et al. (2000) for the Equatorial Pacific. The lack of relationship observed between $PO^{14}CP$ and DCR is considered to be related to the small variability presented by DCR compared to primary production rates (Aristegui and Harrison, 2002; Duarte and Agustí, 1998; del Giorgio and Duarte, 2002) and to the fact that DCR rates include both autotrophic and heterotrophic respiration.

In spite of the fact that respiration rates may have been overestimated due to temperature effects, we measured a positive NCP in the Equatorial Atlantic. Few direct measurements of net microplankton community metabolism have been reported in this area. González et al. (2002) visited 5 stations within 10°N–l0°S in May and October 1997. They found gross primary production (GPP) to exceed respiration at 3 stations, whereas a balanced metabolism took place at the remaining 2 stations. A net heterotrophic community metabolism was consistently found by Serret et al. (2001) in the eastern Equatorial Atlantic waters close to the Gulf of Guinea in May 1998 although the equatorial divergence was not sampled in their study. Yet, estimations from empirical models (Williams, 1998; Duarte et al., 1998; Serret et al., 2002) predict GPP/DCR ratios $\geqslant 1$ in the equatorial upwelling area from our GPP measurements above 100 mmol $O_2\,m^{-2}\,d^{-1}$ between 2°N and 5°S. The contrasting net community production (NCP) values reported by this small number of direct studies and predictions probably reflect the effect of the spatial variability imposed by the cruise tracks, as well as the effect of changing upwelling intensity on biological processes in the Equatorial Atlantic.

According to conceptual models (Legendre and Le Fèvre, 1989, 1991, 1995; Legendre and Rassoulzadegan, 1995) and field observations (Tamigneaux et al., 1999; Pesant et al., 1998; Teira et al., 2001) that link phytoplankton biomass and production to carbon cycling pathways, in pico-

plankton-dominated systems it could be expected that most of the primary production was recycled into the euphotic layer by the microbial food web thus leading to high rates of DCR. However, during this study we observed that the injection of nutrients into the euphotic layer, presumably during periods longer than 2 weeks, was not accompanied by either an important increase in phytoplankton biomass or a change in phytoplankton size-structure or a relative decrease in microbial respiration. Nonetheless, the relative constancy of the microbial community respiration with respect to primary production translated into a three-fold variation of net community metabolism between the TTS and divergence areas, with a primary production to respiration ratio $>2$ in the latter. The fate of the positive NCP measured in the Equatorial Atlantic must be export to either deeper waters, adjacent systems, or higher trophic levels. Sediment trap measurements in the Equatorial Atlantic indicate that organic carbon export amounts on average to 20% of total primary production at 100 m depth (Wefer and Fischer, 1993), and modelling studies for the same region (Thomas et al., 1995) suggested that $20 \pm 10\%$ of the total organic carbon produced is exported from the surface in dissolved form. If the above estimations were applicable to our data, export of organic carbon to deep waters would account for about 40% of the NCP measured in this study, thus suggesting that horizontal transport of particulate and dissolved organic carbon or export to higher trophic levels might be of relevance in this oceanic region. In this connection, Wefer and Fischer (1993) found a latitudinal trend in the rates of vertical particle flux probably related to the existence of horizontal transport of biogenic matter, i.e. the organic matter originated in the equatorial high production tongue, which can be prevented from sinking in situ due to the upwards motion of water, would be transported by the upwelling cell and accumulated at the surface in the convergence boundaries. In addition, export of organic carbon to higher trophic levels, although not measured in this investigation, is likely to be of considerable magnitude given the significant role of mesozooplankton in controlling the microplankton community dynamics in this region as shown in the present study (see above), and the importance of C export through consumption of mesozooplankton by larger metazoans reported for the Equatorial Pacific (Richardson et al., 2004). Further understanding of the patterns of organic matter cycling mediated by higher planktonic trophic levels appears necessary to constrain regional C budgets and estimating the potential C export from the Equatorial Atlantic.

In conclusion, we have found that the equatorial divergence region of the Atlantic Ocean exhibits a positive microbial net community metabolism during autumn, which contrasts with previous measurements in this region (González et al., 2002; Serret et al., 2001) but agrees with the outcome of empirical models which are exclusively based on the rate of photosynthesis as the controlling variable. Despite the fact that the enhanced nutrient supply to the photic layer gave way to significant increases in $^{14}C$ primary production and net community production, the phytoplankton size-structure was still characterized by a dominance of picophytoplankton biomass and productivity. This pattern agrees with the observations of Marañón et al. (2003) in the oligotrophic ocean, who concluded that the microbial community tends to respond to environmental forcing with changes in metabolic rates rather than in trophic organization. Our measurements of a net autotrophic metabolism of the microbial plankton community in the Equatorial Atlantic highlight the importance of nutrient supply in controlling the balance between photosynthesis and respiration in the open ocean.

## Acknowledgements

This study was supported by the UK Natural Environment Research Council through the Atlantic Meridional Transect programme (NER/O/S/2001/00680) and by the Spanish Ministerio de Ciencia y Tecnología (MCyT) through project CIRCANA (MAR1999-1072-C03-01). V.P. was supported by a PFPI fellowship from the MCyT. We are indebted to the captain and crew of the RRS James Clark Ross during the AMT 11 cruise. We acknowledge the collaboration of Begoña

Castro during sampling and experimentation with bacteria and the assistance of Jorge Lorenzo in the laboratory work. Comments by three anonymous reviewers helped in improving an earlier version of the manuscript. This is contribution number 86 of the AMT programme.

## References

Agustí, S., Duarte, C.M., 1999. Phytoplankton chlorophyll-*a* distribution and water column stability in the central Atlantic Ocean. Oceanologica Acta 22 (2), 193–203.

Aiken, J., Rees, N., Hooker, S., Holligan, P., Bale, A., Robins, D., Moore, G., Harris, R., Pilgrim, D., 2000. The Atlantic Meridional Transect: overview and synthesis of data. Progress in Oceanography 45 (3–4), 257–312.

Aristegui, J., Harrison, W.G., 2002. Decoupling of primary production and community respiration in the ocean: implications for regional carbon studies. Aquatic Microbial Ecology 29, 199–209.

Barber, R.T., Sanderson, M.P., Lindley, S.T., Chai, F., Newton, J., Trees, C.C., Foley, D.G., Chavez, F.P., 1996. Primary productivity and its regulation in the equatorial Pacific during and following the 1991–1992 El Niño. Deep-Sea Research II 43 (4–6), 933–969.

Bauerfeind, E., 1987. Primary production and phytoplankton biomass in the equatorial region of the Atlantic at 22°W. Oceanologica Acta no SP, 131–136.

Bender, M., Orchado, J., Dickson, M.L., Barber, R., Lindley, S., 1999. In vitro $O_2$ fluxes compared with $^{14}C$ production and other rate terms during JGOFS Equatorial Pacific experiment. Deep-Sea Research I 46, 637–654.

Benson, B.B., Krause Jr., D., 1984. The concentration and isotopic fractionation of oxygen dissolved in freshwater and seawater in equilibrium with the atmosphere. Limnology and Oceanography 29, 620–632.

Bjørnsen, P.K., Kuparinen, J., 1991. Determination of bacterioplankton biomass, net production and growth efficiency in the Southern Ocean. Marine Ecology Progress Series 71, 185–194.

Brewer, P.G., Riley, J.P., 1965. The automatic determination of nitrate in seawater. Deep-Sea Research 12, 765–772.

Campbell, L., Nolla, H.A., Vaulot, D., 1994. The importance of *Prochlorococcus* to community structure in the central North Pacific Ocean. Limnology and Oceanography 39, 954–961.

Chavez, F.P., Strutton, P.G., Friederich, G.E., Feely, R.A., Feldman, G.C., Foley, D.G., McPhaden, M.J., 1999. Biological and Chemical Response of the Equatorial Pacific Ocean to the 1997–98 El Niño. Science 286, 2126–2131.

del Giorgio, P.A., Duarte, CM., 2002. Respiration in the open ocean. Nature 420, 379–384.

Duarte, C.M., Agustí, S., 1998. The $CO_2$ balance of unproductive aquatic ecosystems. Science 281, 234–236.

Dugdale, R.C., Wilkerson, F.P., 1998. Silicate regulation of new production in the equatorial Pacific upwelling. Nature 391, 270–273.

Eppley, R.W., 1972. Temperature and phytoplankton growth in the sea. Fishery Bulletin 70, 1063–1085.

Franck, V.M., Bruland, K.W., Hutchins, D.A., Brzezinski, M.A., 2003. Iron and zinc effects on silicic acid and nitrate uptake kinetics in three high-nutrient, low-chlorophyll (HNLC) regions. Marine Ecology Progress Series 252, 15–33.

Fernández, E., Marañón, E., Morán, X.A.G., Serret, P., 2003. Potential causes for the unequal contribution of picophytoplankton to total biomass and productivity in oligotrophic waters. Marine Ecology Progress Series 254, 101–109.

González, N., Anadón, R., Marañón, E., 2002. Large-scale variability of planktonic net community metabolism in the Atlantic Ocean: importance of temporal changes in oligotrophic subtropical waters. Marine Ecology Progress Series 233, 21–30.

Grasshoff, K., 1976. Methods of Seawater Analysis. Verlag Chemie, Weinheim, pp. 317

Harrison, W.G., Harris, L.R., 1986. Isotope-dilution and its effects on measurements of nitrogen and phosphorus uptake by oceanic microplankton. Marine Ecology Progress Series 27, 253–261.

Herbland, A., Le Bouteiller, A., 1982. The meanders of equatorial currents in the Atlantic Ocean: influence on the biological processes. Océanographie Tropicale 17 (1), 15–25.

Herbland, A., Voituriez, B., 1979. Hydrological structure analysis for estimating the primary production in the tropical Atlantic Ocean. Journal of Marine Research 37, 87–101.

Herbland, A., Le Borgne, R., Le Bouteiller, A., Voituriez, B., 1983. Structure hydrologique et production primaire dans l'Atlantique tropical oriental. Océanographie Tropicale 18 (2), 249–293.

Herbland, A., Le Bouteiller, A., Raimbault, P., 1985. Size structure of phytoplankton biomass in the Equatorial Atlantic Ocean. Deep-Sea Research 32 (7), 819–836.

Herbland, A., Le Bouteiller, A., Raimbault, P., 1987. Does the nutrient enrichment of the equatorial upwelling influence the size structure of phytoplankton in the Atlantic Ocean? Oceanologica Acta no SP, 115–120.

Huskin, I., Anadón, R., Woodd-Walker, R.S., Harris, R.P., 2001. Basin-scale latitudinal patterns of copepod grazing in the Atlantic Ocean. Journal of Plankton Research 23 (12), 1361–1371.

Isla, J.A., Llope, M., Anadón, R., 2004. Size-fractionated mesozooplankton biomass, metabolism and grazing along a 50°N to 30°S transect of the Atlantic Ocean. Journal of Plankton Research 26, 1301–1313.

Kiorbøe, T., 1993. Turbulence, phytoplankton cell size, and the structure of pelagic food webs. Advances in Marine Biology 29, 1–72.

Kirchman, D.L., 1993. Leucine incorporation as a measure of biomass production by heterotrophic bacteria. In: Kemp,

P.F., Sherr, B.F., Sherr, E.B., Cole, J.J. (Eds.), Handbook of Methods in Aquatic Microbial Ecology. Lewis Publishers, Boca Raton, FL, pp. 509–512.

Kirchman, D.L., Ducklow, H.W., 1993. Estimating conversion factors for the thymidine and leucine methods for measuring bacterial production. In: Kemp, P.F., Sherr, B.F., Sherr, E.B., Cole, J.J. (Eds.), Handbook of Methods in Aquatic Microbial Ecology. Lewis Publishers, Boca Raton, FL, pp. 513–517.

Kirkwood, D., 1989. Simultaneous determination of selected nutrients in sea water. International Council for the Exploration of the Sea (ICES), CM 1989/C:29.

Laws, E.A., Landry, M.R., Barber, R.T., Campbell, L., Dickson, M.L., Marra, J., 2000. Carbon cycling in primary production bottles incubations: inferences from grazing experiments and photosynthetic studies using $^{14}C$ and $^{18}O$ in the Arabian Sea. Deep-Sea Research II 47, 1339–1352.

Le Borgne, R., 1981. Relationships between the hydrological structure, chlorophyll and zooplankton biomasses in the Gulf of Guinea. Journal of Plankton Research 3 (4), 577–592.

Le Borgne, R., Feely, R.A., Mackey, D.J., 2002. Carbon fluxes in the equatorial Pacific: a synthesis of the JGOFS programme. Deep-Sea Research II 49, 2425–2442.

Le Bouteiller, A., Blanchot, J., Rodier, M., 1992. Size distribution patterns of phytoplankton in the western Pacific: towards a generalization for the tropical open ocean. Deep-Sea Research 39 (5), 805–823.

Lefèvre, D., Bentley, T.L., Robinson, C., Blight, S.P., Williams, P.J., le, B., 1994. The temperature response of gross and net community production and respiration in time-varying assemblages of temperate marine micro-plankton. Journal of Experimental Marine Biology and Ecology 184, 201–215.

Legendre, L., Le Fèvre, J., 1989. Hydrodynamic singularities as controls of recycled versus export production in oceans. In: Berger, W.H., Smetacek, V.S., Wefer, G. (Eds.), Productivity of the Ocean: Present and Past. Wiley, Dahlem Konferenzen, pp. 49–63.

Legendre, L., Le Fèvre, J., 1991. From individual cells to pelagic marine ecosystems and to global biogeochemical cycles. In: Demers, S. (Ed.), Particle Analysis in Oceanography. Springer, Heidelberg, pp. 261–300.

Legendre, L., Le Fèvre, J., 1995. Microbial food webs and the export of biogenic carbon in oceans. Aquatic Microbial Ecology 9, 69–77.

Legendre, L., Rassoulzadegan, F., 1995. Plankton and nutrient dynamics in marine waters. Ophelia 41, 153–172.

Leynaert, A., Tréguer, P., Lancelot, C., Rodier, M., 2001. Silicon limitation of biogenic silica production in the Equatorial Pacific. Deep-Sea Research I 48, 639–660.

Longhurst, A., 1993. Seasonal cooling and blooming in the tropical oceans. Deep-Sea Research I 40 (11–12), 2145–2165.

Longhurst, A., 1998. Ecological Geography of the Sea. Academic Press, San Diego, pp. 398.

Marañón, E., Holligan, P.M., Varela, M., Mouriño, B., Bale, A.J., 2000. Basin-scale variability of phytoplankton biomass, production and growth in the Atlantic Ocean. Deep-Sea Research I 47, 825–857.

Marañón, E., Holligan, P.M., Barciela, R., González, N., Mouriño, B., Pazó, M.J., Varela, M., 2001. Patterns of phytoplankton size-structure and productivity in contrasting open ocean environments. Marine Ecology Progress Series 216, 43–56.

Marañón, E., Behrenfeld, M.J.R., González, N., Mouriño, B., Zubkov, M.V., 2003. High variability of primary production in oligotrophic waters of the Atlantic Ocean: uncoupling from phytoplankton biomass and size structure. Marine Ecology Progress Series 257, 1–11.

Minas, M., Herbland, A., Ramade, A., 1983. La production primaire dans les structure hydrologiques de la divergence équatoriale en saison d'upwelling. Océanographie Tropicale 18 (2), 319–329.

Monger, B., McClain, C., Murtugudde, R., 1997. Seasonal phytoplankton dynamics in the eastern tropical Atlantic. Journal of Geophysical Research 102 (C6), 12389–12411.

Morán, X.A.G., Fernández, E., Pérez, V., 2004. Size-fractionated primary production, bacterial production and net community production in subtropical and tropical domains of the oligotrophic NE Atlantic in autumn. Marine Ecology Progress Series 274, 17–29.

Murray, J.W., Barber, R.T., Roman, M.R., Bacon, M.P., Feely, R.A., 1994. Physical and biological controls on carbon cycling in the Equatorial Pacific. Science 266, 58–65.

Murray, J.W., Johnson, E., Garside, C., 1995. A U.S. JGOFS Process Study in the equatorial Pacific (EqPac): introduction. Deep-Sea Research II 42 (2–3), 275–293.

Norland, S., Heldal, M., Tumyr, O., 1987. On the relation between dry matter and volume of bacteria. Microbial Ecology 13, 95–103.

Oudot, C., 1983. La distribution des sels nutritifs ($NO_3$–N-$O_2$–$NO_3$–$NH_4$–$PO_4$–$SiO_3$) dans l'Océan Atlantique intertropical oriental (región du Golfe de Guinée). Océanographie Tropicale 18 (2), 223–248.

Oudot, C., Morin, P., 1987. The distribution of nutrients in the Equatorial Atlantic: relation to physical processes and phytoplankton biomass. Oceanologica Acta no SP, 121–130.

Oudot, C., Gerard, R., Morin, P., Gningue, I., 1988. Precise shipboard determination of dissolved oxygen (Winkler procedure) for productivity studies with a commercial system. Limnology and Oceanography 33 (1), 146–150.

Pesant, S., Legendre, L., Gosselin, M., Ashjian, C., Booth, B., Daly, K., Fortier, L., Hirche, H.J., Michaud, J., Smith, R.E.H., Smith, S., Smith Jr., W.O., 1998. Pathways of carbon cycling in the euphotic zone: the fate of large-sized phytoplankton in the Northeast Water Polynya. Journal of Plankton Research 20, 1267–1291.

Pomeroy, L.R., Sheldon, J.E., Sheldon Jr., W.M., 1994. Changes in bacterial numbers and leucine assimilation during estimations of microbial respiratory rates in seawater by the precision Winkler method. Applied and Environmental Microbiology 60, 328–332.

Porter, K.G., Feig, Y.S., 1980. The use of DAPI for identifying and counting aquatic microflora. Limnology and Oceanography 25, 943–948.

Ragueneau, O., Chauvaud, L., Leynaert, A., Thouzeau, G., Paulet, Y.M., Bonnet, S., Lorrain, A., Grall, J., Corvaisier, R., Le Hir, M., Jean, F., Clavier, J., 2002. Limnology and Oceanography 47 (6), 1849–1854.

Raven, J.A., 1998. The twelfth Tansley Lecture. Small is beautiful: the picophytoplankton. Functional Ecology 12, 503–513.

Richardson, T.L., Jackson, G.A., Ducklow, H.W., Roman, M.R., 2004. Carbon fluxes through food webs of the eastern equatorial Pacific: an inverse approach. Deep-Sea Research I 51, 1245–1274.

Riegman, R., Kuipers, B.R., Noordeloos, A.A.M., Witte, H.J., 1993. Size-differential control of phytoplankton and the structure of plankton communities. Netherlands Journal of Sea Research 31 (3), 255–265.

Robinson, C., Serret, P., Tilstone, G., Teira, E., Zubkov, M.V., Rees, A.P., Woodward, E.M.S., 2002. Plankton respiration in the eastern Atlantic Ocean. Deep-Sea Research I 49, 787–813.

Serret, P., Robinson, C., Fernández, E., Teira, E., Tilstone, G., 2001. Latitudinal variation of the balance between plankton photosynthesis and respiration in the eastern Atlantic Ocean. Limnology and Oceanography 46 (7), 1642–1652.

Serret, P., Fernández, E., Robinson, C., 2002. Biogeographic differences in the net ecosystem metabolism of the open ocean. Ecology 83 (11), 3225–3234.

Signorini, S.R., Murtugudde, R.G., McClain, C.R., Christian, J.R., Picaut, J., Busalacchi, A.J., 1999. Biological and physical signatures in the tropical and subtropical Atlantic. Journal of Geophysical Research 104 (C8), 18367–18382.

Smith, D.C., Azam, F., 1992. A simple, economical method for measuring bacterial protein synthesis rates in seawater using $^{3}$H-leucine. Marine Microbial Food Webs 6, 107–114.

Taylor, A.H., Geider, R.J., Gilbert, F.J.H., 1997. Seasonal and latitudinal dependencies of phytoplankton carbon-to-chlorophyll ratios: results of a modelling study. Marine Ecology Progress Series 152, 51–66.

Tamigneaux, E., Legendre, L., Klein, B., Mingelbier, M., 1999. Seasonal dynamics and potential fate of size-fractionated phytoplankton in a temperate nearshore environment (western Gulf of St. Lawrence, Canada). Estuarine, Coastal and Shelf Science 48, 253–269.

Teira, E., Serret, P., Fernández, E., 2001. Phytoplankton size-structure, particulate and dissolved organic carbon production and oxygen fluxes through microbial communities in the NW Iberian coastal transition zone. Marine Ecology Progress Series 219, 65–83.

Thomas, C., Cauwet, G., Minster, J.F., 1995. Dissolved organic carbon in the equatorial Atlantic Ocean. Marine Chemistry 49, 155–169.

Tomczak, M., Godfrey, J.S., 1994. Regional Oceanography: An Introduction. Pergamon, New York, pp. 422.

Varela, M.M., Bode, A., Fernández, E., Gónzalez, N., Kitidis, V., Varela, M., Woodward, E.M.S., submitted for publication. Latitudinal patterns of nitrogen uptake and dissolved organic nitrogen release in the Central Atlantic Ocean: the role of phytoplankton size-structure. Deep-Sea Research I.

Wefer, G., Fischer, G., 1993. Seasonal patterns of vertical particle flux in equatorial and coastal upwelling areas of the eastern Atlantic. Deep-Sea Research I 40, 1613–1645.

Williams, P.J., le, B., 1998. The balance of plankton respiration and photosynthesis in the open oceans. Nature 394, 55–57.

Woodward, E.M.S., 1994. Nutrient Analysis Techniques. Plymouth Marine Laboratory, 26pp.

Zubkov, M.V., Sleigh, M.A., Tarran, G.A., Burkill, P.H., Leakey, R.J.G., 1998. Picoplanktonic community structure on an Atlantic transect from 50°N to 50°S. Deep-Sea Research I 45, 1339–1355.

Zubkov, M.V., Sleigh, M.A., Burkill, P.H., Leakey, R.J.G., 2000. Bacterial growth and grazing loss in contrasting areas of North and South Atlantic. Journal of Plankton Research 22 (4), 685–711.

Zubkov, M.V., Sleigh, M.A., Burkill, P.H., Leakey, R.J.G., 2000a. Picoplankton community structure on the Atlantic Meridional Transect: a comparison between seasons. Progress in Oceanography 45, 369–386.